Hyperfine Interact (2015) 232:97–110
DOI 10.1007/s10751-015-1122-3

Influence of Co^{2+} on the structural and magnetic properties of substituted magnetites obtained by the coprecipitation method

A. A. Velásquez · J. P. Urquijo

Published online: 24 February 2015

Abstract In this paper we report the effect of divalent cobalt on the structural and magnetic properties of substituted magnetites, $Fe_{3-x}Co_xO_4$, with γ =Co^{2+}/Fe= 0, 5, 10, 15, 20 and 30 % wt, synthesized by the coprecipitation method. The samples were characterized by Atomic Absorption Spectroscopy, X-ray Diffraction, room temperature Mössbauer Spectroscopy and Vibrating Sample Magnetometry. The effect of Co^{2+} was found to depend strongly of the concentration employed in the synthesis process. For $\gamma \leq 15$ % the Co^{2+} promotes the formation of particles more crystalline and with higher saturation magnetization, remanence and coercivity than those obtained in absence of this cation. A sequential increasing of the lattice parameter is observed, as well as a reduction in the hyperfine magnetic field of the $Fe^{2.5+}$sub spectrum, while the hyperfine magnetic field of the Fe^{3+}sub spectrum keeps almost constant. For γ =20 % and 30 % the crystallinity of the samples decreases, particle size distribution effects are evidenced and the saturation magnetization decreases drastically. The results suggest that for low Co^{2+} contents the substitution of $Fe^{3+}$by Co^{2+} at octahedral sites of the inverse spinel system is the dominant effect, while for the highest concentrations used the substitution of Fe^{2+} by Co^{2+} and the increasing of the particle size distribution are the dominant effects.

Keywords Substituted magnetites · Divalent cobalt · Mössbauer spectroscopy

Proceedings of the 14th Latin American Conference on the Applications of the Mössbauer Effect (LACAME 2014), Toluca, Mexico, 10-14 November 2014

A. A. Velásquez (✉)
Grupo de Electromagnetismo Aplicado, Universidad EAFIT, A.A. 3300, Medellín, Colombia
e-mail: avelas26@eafit.edu.edu.co

J. P. Urquijo
Grupo de Estado Sólido, Instituto de Física, Universidad de Antioquia, A.A. 1226, Medellín, Colombia

1 Introduction

Substituted magnetites $Fe_{3-x}M_xO_4$, where M is a transition metal, are very promissory materials for the development of devices in the macro, micro and nanoscale, such as nanofibers [1], nanocomposites [2], coatings for electromagnetic shieldings [3–5], high dielectric constant capacitors [6], magnetic cores for solenoids and electrical transformers [7], ferrofluids for magneto viscosity experiments [8], magnetic recording media and spintronic devices [9], drug delivery agents [10], among others. In particular, the spinel system $Fe_{3-x}Co_xO_4$ has attracted the attention of many investigators because the Co^{2+} is more stable than Fe^{2+} when it is incorporated in the magnetite structure, preventing changes in the electric and magnetic properties of the material by oxidation effects, its ionic radius is slightly smaller than that of Fe^{2+}, which implies that no drastic changes in the crystalline structure appear when partial substitution of Co^{2+} takes place. When the orbital angular moment of the iron ions is quenched in the structure, the magnetic moment of Co^{2+} is $3\mu_B$ while the magnetic moments of Fe^{2+} and Fe^{3+} are $4\mu_B$ and $5\mu_B$ respectively, which means that variations in the magnetization of the material are expected if Co^{2+} substitutes Fe^{2+}, Fe^{3+}or both cations in the crystalline structure. Independently of the type of substitution, the magnetic interactions of the inverse spinel system $Fe_{3-x}Co_xO_4$ are comparable with those of magnetite Fe_3O_4, which makes possible tuning their magnetic and electrical properties according to the Co^{2+} content employed in the synthesis process. In this paper we report the study of divalent cobalt substituted magnetites synthesized by the coprecipitation method, with $\gamma = Co^{2+}/Fe = 0$, 5, 10, 15, 20 and 30 % wt, for exploring the role of this cation on the magnetic and structural properties of the inverse spinel system, looking for future applications of these materials in the development of high performance electromagnetic devices for sensing and actuation stages. Details on the synthesis process, the characterization of the obtained samples and the interpretation of the results are presented in the following sections.

2 Experimental procedure

2.1 Synthesis of the samples

The samples were synthesized by the coprecipitation method described by Cornell and Schwertmann [11]. $FeCl_2$-$4H_2O$ and $FeCl_3$-$6H_2O$ were employed as Fe^{2+} and Fe^{3+}precursors, respectively, $CoCl_2$-$6H_2O$ was employed as Co^{2+} precursor and KOH was employed to carry out the formation of metal complexes. All reagents employed were of analytical grade, Merck KGaA. In order to test the efficiency of the method to obtain only spinel phase in the final products, as well as to have a reference sample to evaluate the effect of the Co^{2+} on the samples, a nonsubstituted magnetite was synthesized by preparing aqueous solutions 0.17 M (50 ml) $FeCl_2$-$4H_2O$, 0.35 M (50 ml) $FeCl_3$-$6H_2O$ and 1.38 M (50 ml) KOH. The weights of the salts $FeCl_2$-$4H_2O$ and $FeCl_3$-$6H_2O$ were calculated to have a ratio Fe^{3+}/Fe^{2+} =2/1 in the starting solutions, looking for a stoichiometric magnetite. The solutions of $FeCl_2$-$4H_2O$ and $FeCl_3$-$6H_2O$ were mixed in a glass reactor, under constant bubbling with $N_{2(g)}$, magnetic stirring at 600 rpm and controlled temperature at 90 °C. A system for temperature control and magnetic stirring IKA RCT was employed for this purpose. When the temperature reached 90 °C, 50 ml of the alkaline solution of KOH were added dropwise to the mixture during 30 min, then the reaction continued at 90 °C during 30 min with vigorous stirring and deaeration. Finally the reactor was kept at rest for 12 h while room temperature was reached and the black precipitate observed at the bottom of

the reactor. The precipitate was repeatedly washed with deionized water to obtain a neutral pH in the residual supernatant. Finally the precipitate was filtered and dried in an oven at 40 °C for 48 h. The substituted magnetites were prepared by adding a third aqueous solution of $CoCl_2$-$6H_2O$ (50 ml) to the mixture of solutions of $FeCl_2$-$4H_2O$ and $FeCl_3$-$6H_2O$ before described, in the following concentrations: 2.45×10^{-2} M, 4.90×10^{-2} M, 7.35×10^{-2} M, 9.80×10^{-2} M and 1.47×10^{-1} M for $\gamma = Co^{2+}/Fe = 5$ %, 10 %, 15 %, 20 % and 30 % % wt, respectively. The subsequent procedure was the same as described for the nonsubstituted magnetite.

2.2 Experimental techniques

Atomic Absorption Spectroscopy measurements were performed with an UNICAM 929 AA spectrometer with cobalt lamp; the samples were first solubilized in HCl solutions and then diluted in water to keep the cobalt concentrations within the linear region of quantification. X-ray diffractograms were taken with a PANalytical X'Pert PRO diffactometer, with Cu-K_α radiation (λ =1.540598 A°), angular range 2θ:15° -85° , step of 0.016° and counting time of 1s per step. Room temperature Mössbauer spectra were taken with a multichannel analyzer developed in our laboratory, which operates with a ^{57}Co/Rh (25 mCi) radioactive source, 512 channels and a triangular velocity waveform. Thin absorbers with disk shape and effective thickness of 6 mg/cm^2 of iron were prepared for these measurements. Room temperature hysteresis loops were taken with a Physical Property Measurement System 6000 PPMS from Quantum Design. The range of magnetic field used was 2×10^4 Oe in steps of 50 Oe.

3 Results and discussion

3.1 Atomic absorption measurements

The percentages of cobalt per total weight of sample ($\mathbf{Co^{2+}/W_{Total}}$) are presented in Table 1. The expected cobalt weight percentages calculated theoretically from the precursor solutions are also included for comparison. It can be observed that the cobalt concentration increases as the ratio $\gamma = Co^{2+}/Fe$ increases in the precursor solutions, however the contents found are significantly lower than those obtained theoretically, specially for γ =5 %, 10 % and 15 %, where the contents are lower than 66 % of the expected values. The content of cobalt for the samples with γ =20 % and 30 % is closer to the expected value, indicating that Co^{2+} substitution is more efficient than 80 % for $\gamma > 20$ % for the synthesis conditions employed by us. We propose two possible mechanisms for explaining the low incorporation of Co^{2+} at low doping, the first one is that the coprecipitation method produces very small particles, where the relation surface to volume is significant. If the Co^{2+} has preference to occupy the volume of the particles instead their surface, a poor efficiency of substitution is expected when small particles are formed. When the particle size increases with increasing content of Co^{2+} in the precursor solution, more Co^{2+} can keep into the volume, improving the efficiency of substitution. The second mechanism is that, as we will see later, if the Co^{2+} interferes with the crystallization at high concentrations, these ions can keep trapped between the pores of the particles via mechanical trapping [12], which can increase the final population of cobalt found in the products, being this process less probable at low concentrations, where the crystallization process, according to XRD measurements seems to be better.

Table 1 Weight percentage of cobalt found in the substituted magnetites

γ = Co^{2+}/Fe (% wt)	$Co^{2+}/W_{Total-measured}$ (% wt)	$Co^{2+}/W_{Total-theor}$ (% wt)
5	1.6 ± 0.1	3.4
10	3.7 ± 0.2	6.6
15	6.2 ± 0.2	9.4
20	9.7 ± 0.6	12.1
30	14.5 ± 0.3	16.8

3.2 X-ray diffraction

The X-ray diffractograms of the samples are presented in Fig. 1. The diffractograms were processed with the software Powder X [13] in order to remove the continuous background signal of the tube and for obtaining the position of the peaks, the full width at half maximum of peak **FWHM** and indexing of peaks. Only cubic inverse spinel phase was identified in all patterns, which can be corroborated by the sequence of peaks indexed.

Table 2 shows the structural parameters derived from the X-ray diffractograms. For the samples with $\gamma \leq 15$ % is evident the shift left of the position of the main peak due to the reflections in the planes (311), indicating an expansion of the lattice parameter, **a**, of the crystals as the Co^{2+} content increases. This behavior has been reported in the literature by Hua and coworkers [2] in nanocomposites of nonstoichiometric cobalt ferrites obtained by the sol gel method, and by Zhang and coworkers [14] in cobalt ferrites obtained by solid state reaction sintering at atmospheric pressure, being attributed to substitution of Fe^{3+} by Co^{2+}, because the ionic radius of Co^{2+}(0.74A°) is higher than the ionic radius of Fe^{3+} (0.64A°). The substitution of Fe^{2+}(0.76A°) by Co^{2+} is not consistent with this effect. For the samples with γ =20 % and 30 % an irregular tendency is observed in the lattice parameter, which decreases for γ =20 % and then increases for γ =30 %. This effect indicates that the substitution Fe^{3+} by $Co^{2+}$is not the dominant mechanism at these concentrations but Fe^{2+} by Co^{2+} substitution, vacancies and structural defects can be introduced. The mean crystallite size, **L**, was estimated by applying the modified Scherrer's equation [15], being their values between 12 and 16 nm. Another important effect observed is that the sample with $\gamma = 5$ % has the lowest value of **FWHM** and the highest value of the mean crystallite size, on the other hand, the intensity $I_{(311)}$ of the main peak for the samples with γ =5, 10 and 15 % wt is higher than that of the nondoped magnetite and the samples with γ =20 and 30 % wt. The higher intensity observed in the three samples with smaller doping is an indication that a major set of planes oriented in the direction [311] are contributing to the signal in the diffractogram, which evidences that the crystallinity of the samples improves with low Co^{2+} contents during the synthesis process.

3.3 Mössbauer spectroscopy

Room temperature Mössbauer spectra of the samples are presented in Fig. 2 and the hyperfine parameters obtained by fitting of the spectra are presented in Table 3. The fitting of the spectra was performed by least square, assuming Lorentzian line profiles in all cases. The software MOSFIT [16] was employed for this purpose and all hyperfine parameters were left free during the fittings. From the Table 3 is evident that for $\gamma \leq 15$ % the Co^{2+} does not have an appreciable effect on the tetrahedral sublattice occupied by Fe^{3+}ions, because

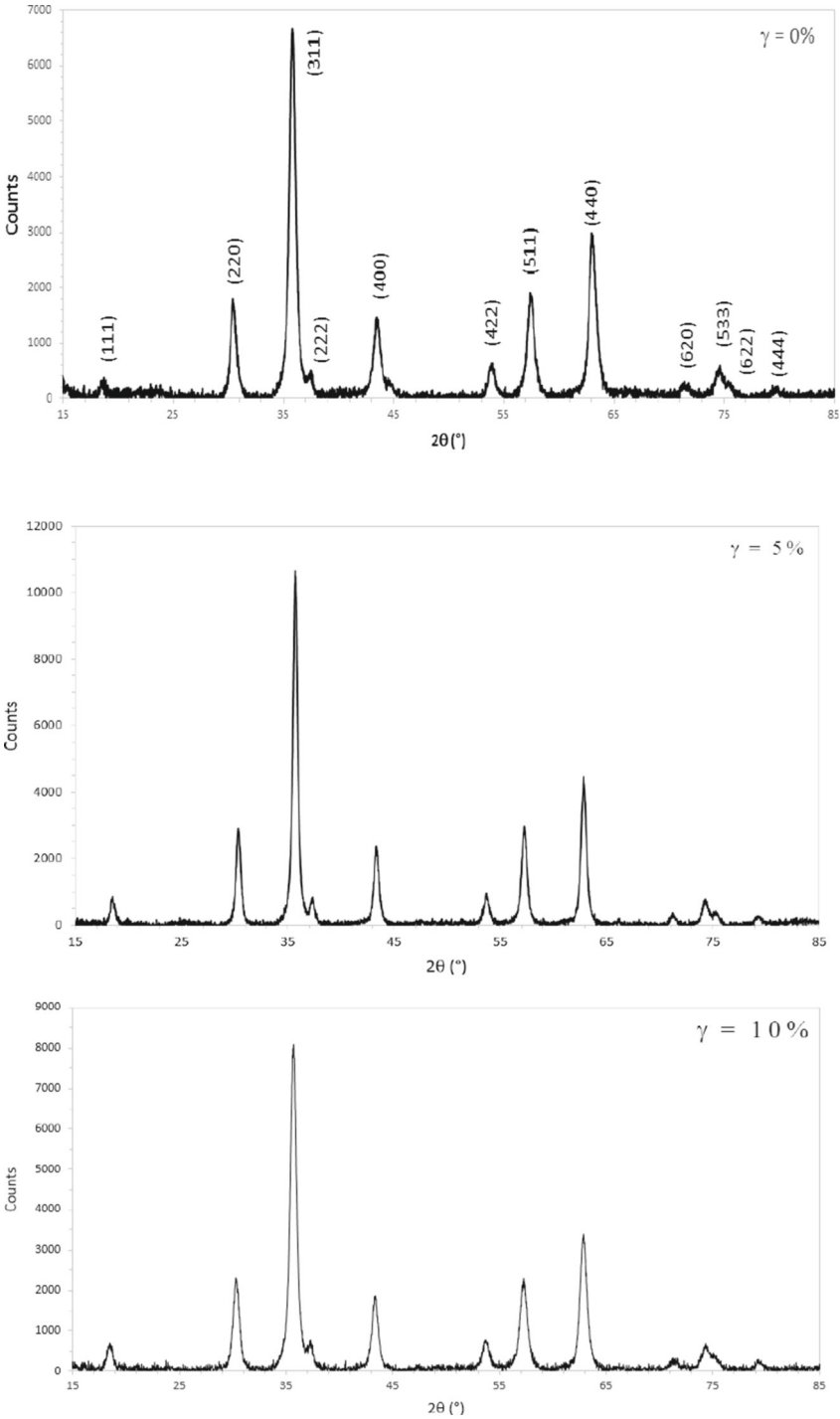

Fig. 1 X-ray diffractograms of the samples

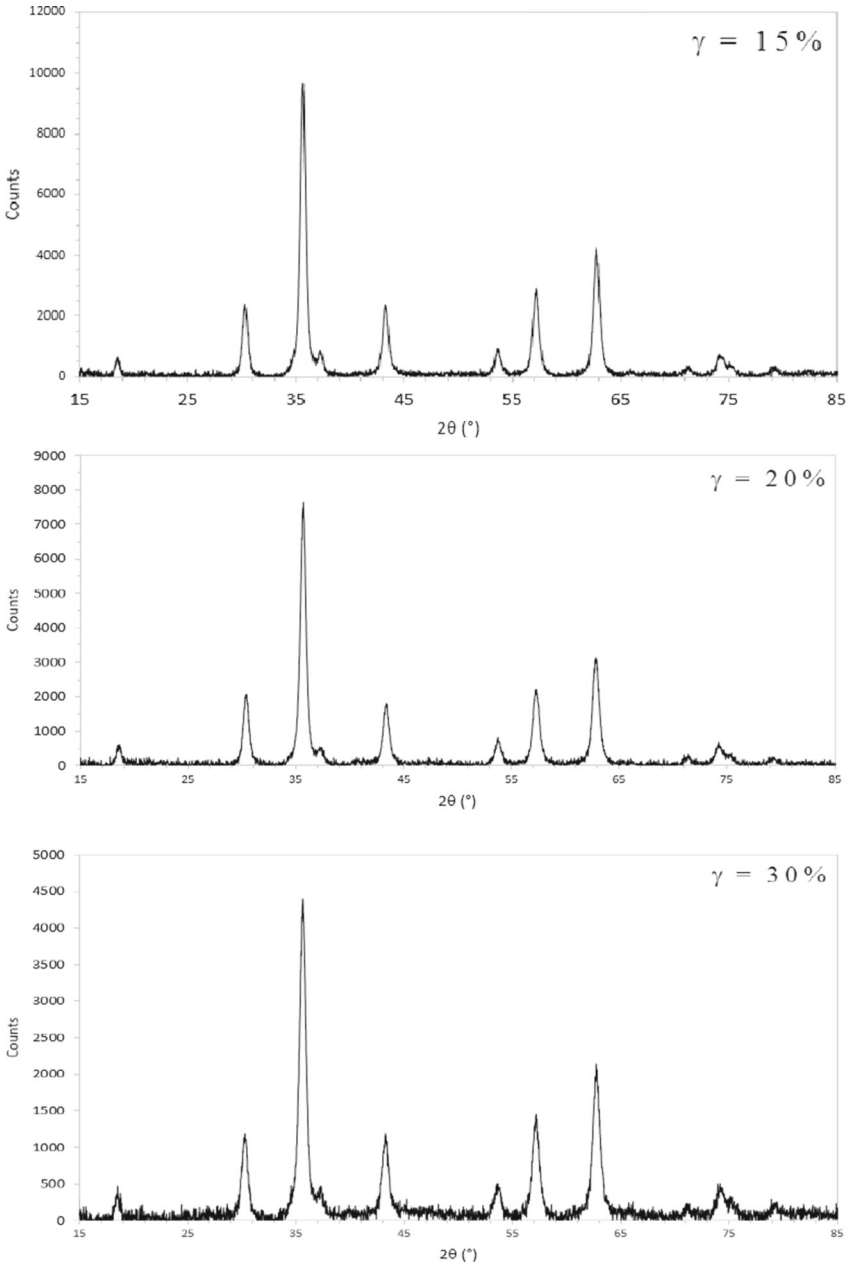

Fig. 1 (continued)

the hyperfine parameters are very similar in all spectra. On the other hand, a more notable tendency is observed in the octahedral sublattice occupied by $Fe^{2.5+}$ ions, whose subspectrum broadens as the Co^{2+} content increases, while the hyperfine magnetic field decreases gradually from $\gamma = 5$ %. The hyperfine magnetic fields in all spectra are lower than those

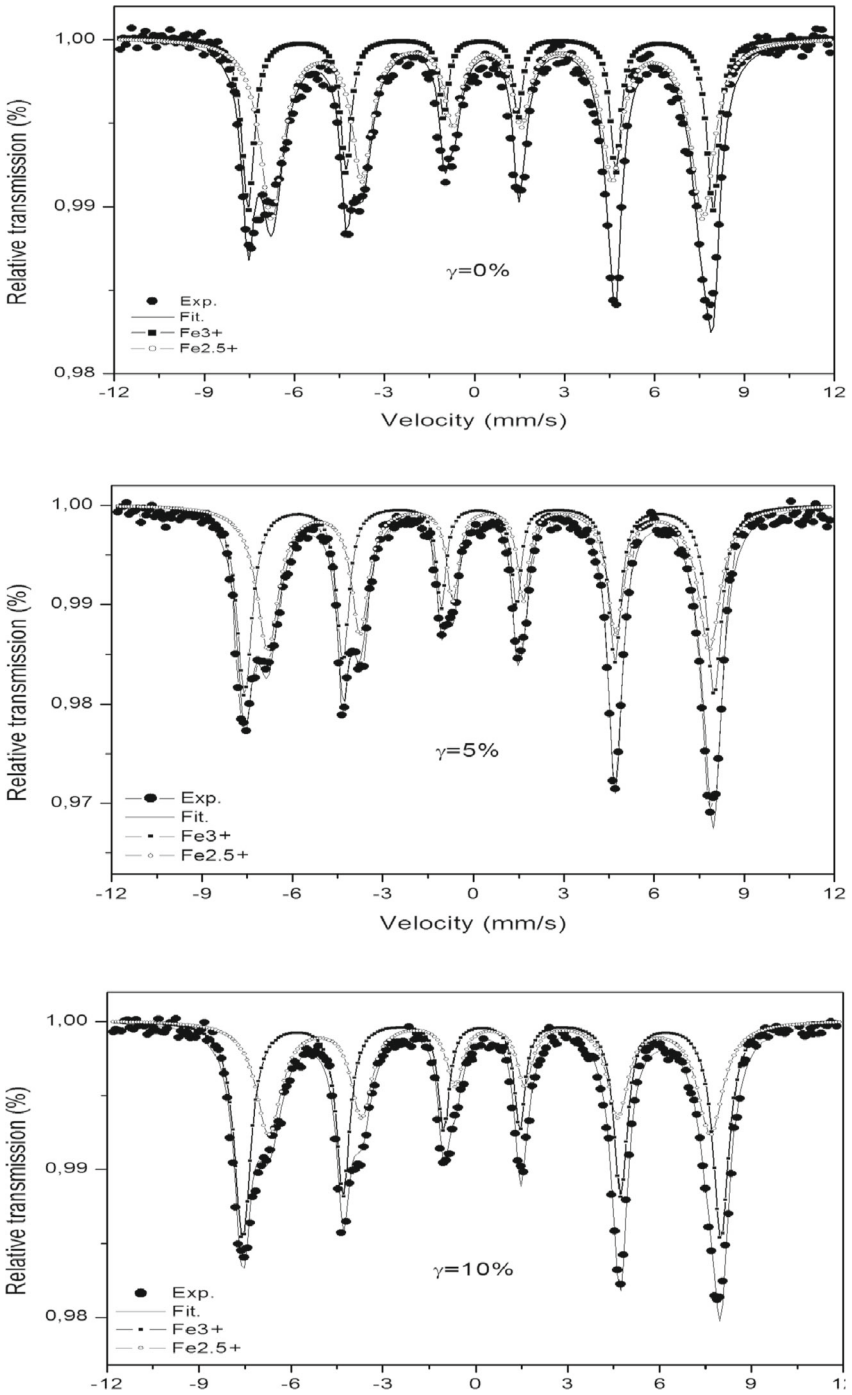

Fig. 2 Room temperature Mössbauer spectra of the samples

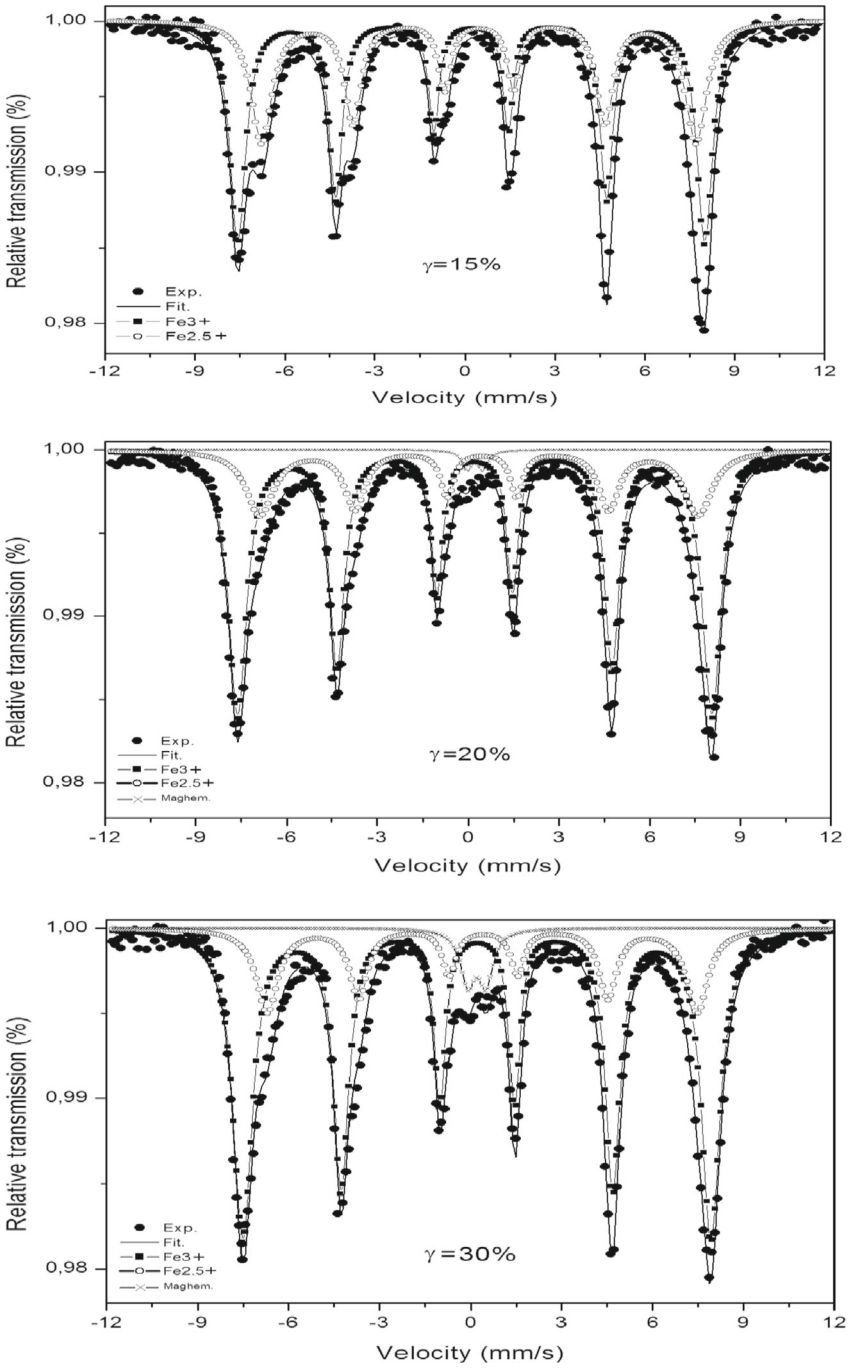

Fig. 2 (continued)

Table 2 Spectral and structural parameters obtained from the X-ray diffractograms

γ = **Co^{2+}/Fe (% wt)**	**$2\theta_{(311)}$(°) ± 0.008**	**$I_{(311)}$(Counts)**	**FWHM(°) ± 0.011**	L(nm)	a(Å)± 0.006
0	35.751	6,637	0.635	12	8.321
5	35.673	10,667	0.504	16	8.341
10	35.651	8,084	0.680	13	8.345
15	35.632	9,640	0.680	12	8.351
20	35.707	7,636	0.595	14	8.331
30	35.665	4,397	0.689	12	8.351

expected for stoichiometric and crystalline magnetites at room temperature, being these approximately 49 T and 46 T for tetrahedral and octahedral sites, respectively, which can be an indication that an important number of vacancies are present in both sites. The generation of vacancies is favored by the low particle size characteristic of the coprecipitation synthesis method [11] because the high ratio surface to volume of the particles facilitates their interaction with the oxygen, with the subsequent oxidation of Fe^{2+} to Fe^{3+}. This oxidation blocks the hopping current between some pair of ions Fe^{2+} and Fe^{3+} occupying neighboring octahedra, locating both ionic states in the structure and therefore increasing the area of the Fe^{3+} subspectrum relative to the area of the $Fe^{2.5+}$subspectrum, where the hopping keeps. The effect of vacancies seems to be more important for the nondoped sample, which presents hyperfine magnetic fields even lower than those of the sample with $\gamma = 5$ %.

From $\gamma = 5$ % is observed a successive decreasing of the hyperfine magnetic field of the $Fe^{2.5+}$ ions occupying the octahedral sublattice, indicating that the magnetic moment experimented by the nuclei of these ions is lowering by the presence of Co^{2+}. This effect is expected if we consider that the electronic configuration of Co^{2+} is $3d^7$, with a magnetic moment $\mu = 3\mu_B$, while that of Fe^{3+} is $3d^5$, with $\mu = 5\mu_B$ and Fe^{2+} is $3d^6$, with $\mu = 4\mu_B$. According to the Yafet-Kittel model for ferrimagnets substituted with transition cations [17], if the substitution of Fe^{3+} by Co^{2+} is dominating at low Co^{2+} contents, a decreasing of the sublattice magnetization at octahedral sites is expected, which explains the simultaneous decreasing of the hyperfine magnetic field in these sites and the increasing of the lattice parameter observed in the X-ray patterns up to γ =15 %.

For $\gamma = 20$ % and 30 % some variation is observed in the hyperfine magnetic field of tetrahedral sites while the magnetic field at octahedral sites continues decreasing. This behavior points a reduction in the superexchange interaction between Fe^{3+}at tetrahedral sites with Fe^{3+} and Fe^{2+}at octahedral sites produced by the entry of the Co^{2+}in the octahedral sublattice. The reduction of the hyperfine magnetic field at octahedral sites is not as strong as that observed at lower concentrations, indicating that substitution of Fe^{3+} by $Co^{2+}$is not dominant at these concentrations but substitution of Fe^{2+} by $Co^{2+}$is the main mechanism. The replacing of Fe^{2+} ($4\mu_B$) by Co^{2+}($3\mu_B$) produces a lower reduction in the hyperfine magnetic field at the octahedral sites than that observed if the replacing is of Fe^{3+}($5\mu_B$) by Co^{2+} ($3\mu_B$). The substitution of Fe^{2+} by Co^{2+} supports the notable decreasing of the isomer shift observed for $\gamma = 20$ % and 30 %, indicating that a lower effective electronic charge is present at the nuclei of $Fe^{2.5+}$ ions, which points that more ferric than ferrous ions are populating the octahedral sublattice for the higher Co^{2+} concentrations used. The notable increasing observed in the spectral linewidth, W, of the spectra of the samples with $\gamma = 20$ % and 30 % is another indication that the natural environment of $Fe^{2.5+}$ions present in the octahedral sublattice is being altered by incorporation

Table 3 Mössbauer parameters of the samples obtained by fitting of the spectra

$\gamma = Co^{2+}/Fe$ (% wt)	Subspectrum	B_{hf}(T) ± 0.2	IS (mm/s) ± 0.02	QS (mm/s) ± 0.02	W (mm/s) ± 0.02	A(%)
0	Fe^{3+}	48.1	0.33	0.00	0.36	38
	$Fe^{2.5+}$	45.0	0.63	0.00	0.57	62
5	Fe^{3+}	48.3	0.31	0.00	0.36	51
	$Fe^{2.5+}$	45.7	0.61	0.01	0.46	49
10	Fe^{3+}	48.3	0.33	0.00	0.42	55
	$Fe^{2.5+}$	44.9	0.58	0.00	0.51	45
15	Fe^{3+}	48.3	0.32	0.00	0.42	59
	$Fe^{2.5+}$	44.6	0.58	0.00	0.55	41
20	Fe^{3+}	48.6	0.32	0.00	0.44	68
	$Fe^{2.5+}$	44.3	0.54	-0.01	0.61	30
	Doublet	−−	0.33	0.53	0.40	2
30	Fe^{3+}	47.9	0.32	0.00	0.43	72
	$Fe^{2.5+}$	44.0	0.50	-0.03	0.73	23
	Doublet	–	0.34	0.62	0.61	5

Convention for the parameters is: B_{hf} hyperfine magnetic field, *IS* isomer shift relative to α-Fe, QS quadrupole splitting, *W* linewidth of the inner lines, *A* spectral area

of Co^{2+}, generating a distribution of hyperfine magnetic fields at these sites. Finally, the doublet observed in the spectra of the samples with γ =20 % and 30 %, which we assign to superparamagnetic maghemite (γ-Fe_2O_3), evidences the formation of smaller particles, with higher size distribution than those obtained in the samples with lower Co^{2+} content, which confirms that Co^{2+} can interfere with the crystallization process of the magnetite particles for the highest concentrations employed in our synthesis.

The absorption percentage, close to 2 %, observed in all Mössbauer spectra is comparable with the value reported for Sorescu and coworkers [18] in Co^{2+}substituted magnetites obtained by the hydrothermal method, however it is lower than the absorption percentage reported by da Costa and coworkers [19] in pure magnetites. In our case, the low absorption could be attributed to a non optimal selection of the 14.4 keV signal in the pulses discriminator of the Mössbauer spectrometer, however the counting statistic of the spectra was significant in order to obtain a satisfactory signal to noise ratio and have a good fitting in all spectra.

3.4 Magnetization measurements

Room temperature hysteresis loops of the samples are presented in Fig. 3, the main parameters extracted from these loops, such as specific saturation magnetization $\mathbf{M_s}$, coercive magnetic field $\mathbf{H_c}$ and remanent magnetization $\mathbf{M_r}$ are reported in Table 4. From the hysteresis loops is notable the low value of the coercive magnetic field and the remanence of the nondoped magnetite, which is an indication that small particles are obtained by the coprecipitation method under the conditions employed by us. An important fraction of these particles could be single domain or even superparamagnetic within the window time of measurement of VSM ($\sim 10^2$ s), however the particles do not exhibit superparamagnetic behavior within the window time of room temperature Mössbauer spectroscopy ($\sim 10^{-8}$ s for ^{57}Fe) because no doublets were observed in the Mössbauer spectrum of this sample.

The small particle effect evidenced in the hysteresis loop of the nondoped sample can also explain why the hyperfine magnetic fields found by Mössbauer spectroscopy at tetrahedral and octahedral sites of this sample, 48.1 T and 45.0 T, respectively are lower than the values of 49 T and 46 T expected for tetrahedral and octahedral sites of a crystalline and stoichiometric magnetite, which occurs because in small particles the net magnetic moment at nuclei of ions Fe^{3+} and $Fe^{2.5+}$ is reduced by the surface anisotropy, which generates a "canting" of the magnetic moments of the ions occupying the surface of the particles, being this surface a considerable fraction of the volume of the particles.

The coercivity, remanence and saturation magnetization of the sample with γ =5 % are higher than those of the nondoped sample, confirming the better crystallinity and higher crystallite size observed by X-ray for this sample, as well as its higher hyperfine magnetic field observed by Mössbauer spectroscopy for tetrahedral and octahedral sites. This fact supports the hypothesis that the Co^{2+} in low concentrations can improve the crystallinity of the samples and promote the formation of larger particles than those obtained without doping in our syntheses.

From γ =15 % a reduction is observed in the saturation magnetization, being the most drastic change for γ =30 %, where M_s =59.5 emu/g, what means a reduction of 32 % from the maximum value of 78.4 emu/g observed for γ =10 %. The significant doublet observed in the Mössbauer spectra of the sample with γ = 30 % evidences the formation of single domain particles, indicating a higher particle size distribution for these concentrations, consistent with the lower crystallinity evidenced in the X-ray pattern of this sample.

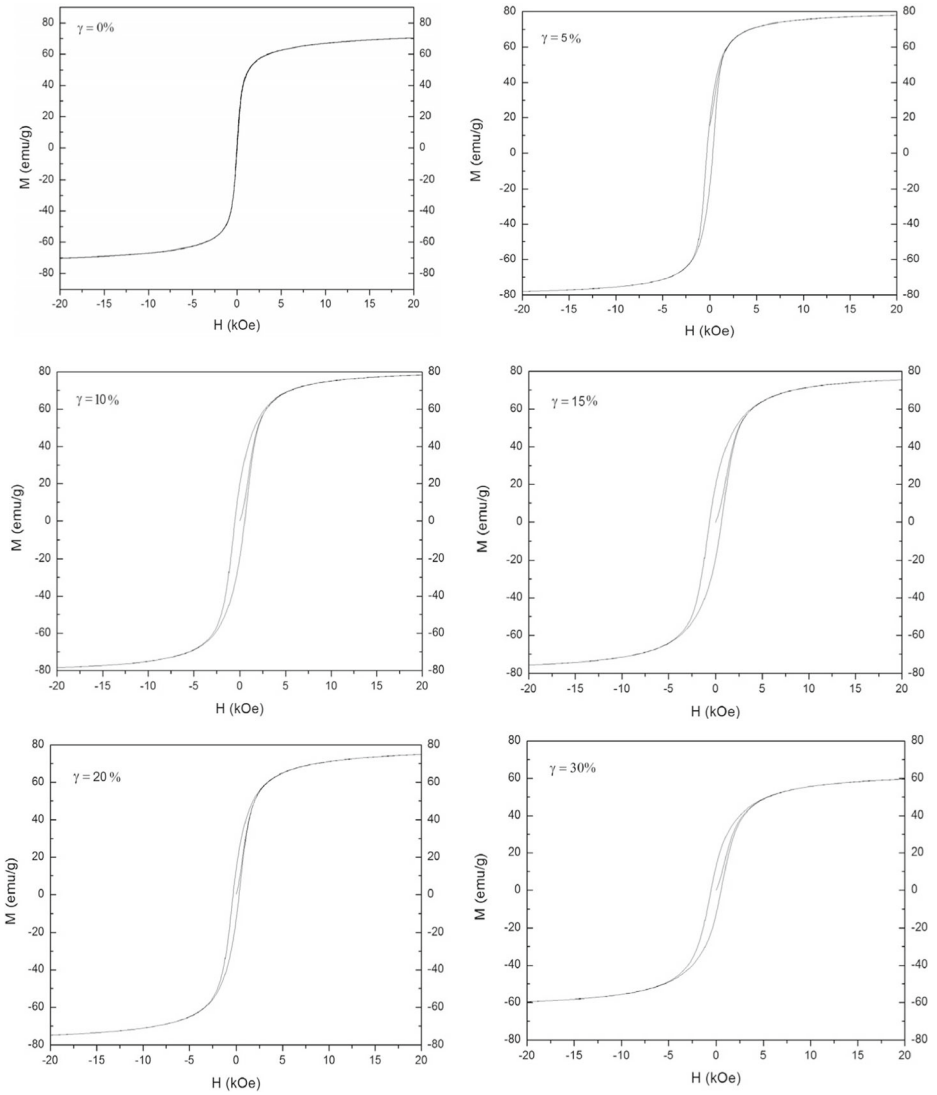

Fig. 3 Room temperature hysteresis loops of the samples

Table 4 Hysteresis parameters of the samples

γ = Co^{2+}/Fe (% wt)	M_s(emu/g)	M_r(emu/g)	H_C(Oe)
0	70.2 ± 0.6	1.18 ± 0.01	50 ± 2
5	78.1 ± 0.5	18.4 ± 0.1	350 ± 2
10	78.4 ± 0.6	19.5 ± 0.2	525 ± 2
15	75.6 ± 0.7	19.4 ± 0.2	650 ± 2
20	74.9 ± 0.7	13.6 ± 0.1	325 ± 2
30	59.5 ± 0.5	12.8 ± 0.1	550 ± 2

4 Conclusions

We synthesized magnetite samples, both pure and substituted with Co^{2+} by the coprecipitation method. Only inverse spinel phase was found in the final products, indicating that Co^{2+} does not promote the formation of other phases different to cubic inverse spinel. The efficiency of cobalt substitution was lower than 66 % for Co^{2+}/Fe= 5 %, 10 % and 15 % and higher than 80 % for Co^{2+}/Fe= 20 % and 30 %, which can be explained either by low entry of Co^{2+} in the structure of small particles with important surface to volume ratio or because more Co^{2+} can keep trapped in the porous of larger but less crystalline particles, resulting in an inhomogeneous efficiency of the substitution of Co^{2+} in the final products according to the doping employed in the precursor solution. From our measurements we can not point which mechanism dominates this effect. Magnetic and structural properties of the products showed a strong dependence with the Co^{2+} content. The presence of Co^{2+} in ratios Co^{2+}/Fe up to 15 % increases the lattice parameter of the crystals and broadens the octahedral subspectrum, indicating a dominant substitution of Fe^{3+} by Co^{2+} in the octahedral sites at low concentrations. On the other hand, low Co^{2+} contents improve the crystallinity of the samples, increase their particle size and their saturation magnetization. For Co^{2+}/Fe $\geq$ 20 % less crystalline samples are obtained, a greater size particle distribution is evidenced and the magnetic interactions are reduced, being a small fraction of the particles in superparamagnetic state at room temperature. According to Mössbauer measurements the Co^{2+} shows major preference for occupying the octahedral sublattice, substituting Fe^{3+} at low contents (Co^{2+}/Fe $<$ 15 % in our syntheses) and mainly Fe^{2+} at the highest Co^{2+} contents employed (Co^{2+}/Fe = 20 %, 30 %). Our study shows that Co^{2+} can improve or worsen the magnetic and structural properties of magnetite according to the concentration used in the coprecipitation method, being its effect more drastic at high concentrations, where it interferes with the crystallization process and decreases the magnetic properties of the magnetite.

References

1. Chen I.-H., Wang C.-C., Chen C.-Y.: Fabrication and characterization of magnetic cobalt ferrite/polyacrylonitrile and cobalt ferrite/carbon nanofibers by electrospinning. Carbon **48**, 604–611 (2010)
2. Hua, J., Liu. M., Wang. L., Xu, S.C., Feng, M., Li, H.B.: Effect of Co^{2+} content on the magnetic properties of $Co_xFe_{3-x}O_4/SiO_2$ nanocomposites. Hyperfine Interact **219**, 41–48 (2013)
3. Bogush, B.: Application of electroless metal deposition for advanced composite shielding materials. J. Optoelectron. Adv. Mater. **7**(3), 1635–1642 (2005)
4. Moon, S.K., Jae, G.K.: Microwave-Absorbing Characteristics of NiCoZn Ferrite Prepared by Using a Co-Precipitation Method. Journal of the Korean Physical Society **53**(2), 737–741 (2008)
5. Praveena, K., Srinath, S.: Synthesis and Characterization of CoFe2O4/Polyaniline Nanocomposites for Electromagnetic Interference Applications. J. Nanosci. Nanotechnol. **14**, 4371–4376 (2014)
6. Kumbhar, V.S., Jagadale, A.D., Shinde, N.M., Lokhande, C.D.: Chemical synthesis of spinel cobalt ferrite ($CoFe_2O_4$) nano-flakes for supercapacitor application. Appl. Surf. Sci. **259**, 39–43 (2012)
7. The International Magnetics Association: Soft Ferrite Cores, A User's Guide. http://www.transformer-assn.org/Soft%20Ferrite%20Cores%20User%20Guide.pdf. Accessed 15 June 2014
8. Felderhof, B.U.: Flow of a ferrofluid down a tube in an oscillating magnetic field. Phys. Review E **64**, 021508-1/021508-7 (2001)
9. Bilecka, I., Kubli, M., Amstad, E., Niederberger, M.: Simultaneous formation of ferrite nanocrystals and deposition of thin films via a microwave-assisted nonaqueous sol–gel process. J. Sol.-Gel. Sci. Technol. **57**, 313–322 (2011)
10. Pankhurst, Q.A., Connolly, J., Jones, S.K., Dobson, J.: Application of magnetic nanoparticles in biomedicine. J. Phys. D: Appl. Phys. **36**, R167–R181 (2003)

11. Cornell, R.M., Schwertmann, U.: The iron oxides, pp. 135, 140. WILEY-VCH Verlag GmbH, D-69469 Weinheim, Germany (2000)
12. Skoog, D.A., West, D.M., Holler, F.J., Crouch, S.R.: Fundamentals of Analytical Chemistry, Ninth Edition. Brooks/Cole, Cengage Learning, pp. 289 (2013)
13. Dong, C.: PowderX: Windows-95-based program for powder X-ray diffraction data processing. J Appl Crystallogr **32**, 168–173 (1999)
14. Zhang, H.G., Zhang, Y.J., Wang, W.H., Wu, G.H.: Origin of the constricted hysteresis loop in cobalt ferrites revisited. J. Magn. Magn. Mater. **323**, 1980–1984 (2011)
15. Monshi, A., Reza Foroughi, M., Reza Monshi, M.: Modified Scherrer Equation to Estimate More Accurately Nano-Crystallite Size Using XRD. World Journal of Nano Science and Engineering **2**, 154–160 (2012)
16. Vandenberghe, R., De Grave, E., De Bakker, P.M.A.: On the methodology of the analysis of Mössbauer spectra. Hyperfine Interact **83**, 29–49 (1994)
17. Willard, M.A., Nakamura, Y., Laughlin, D.E., McHenry, M.E.: Magnetic Properties of Ordered and Disordered Spinel-Phase Ferrimagnets. J. Am. Ceram. Soc. **82 [12]**, 3342–3346 (1999)
18. Sorescu, M., Oberst, T., Gosset, K., Tarabasanu, D., Diamandescu, L.: Direct Evidence for Cobalt Substitution Effects in Magnetite. Solid State Commun. **113**(10), 573–575 (2000)
19. da Costa, G.M., Andujar C.B., De Grave E., Pankhurst Q.: Magnetite, non-stoichiometric magnetite and maghemite: Can they be distinguished by Mössbauer spectroscopy?. ICAME 2013 - International Conference on the Applications of the Mössbauer Effect, Opatija, Croatia, 1-6 September 2013. http://www.icame2013opatija.com/system/file/249/da_Costa_P2.pdf. Accessed 15 December 2014